

Local Electrochemical Investigation of Single Grains of Polycrystalline Cu-16%Zn-8%Al Alloy

José T. C. Barragan,^a Matildes Blanco,^a Nilso Barelli,^a Rodrigo Della Noce,^a
Cecílio S. Fugivara,^a Javier Fernández^b and Assis V. Benedetti^{*a}

^aDepartamento de Físico-Química, Instituto de Química, Universidade Estadual Paulista,
14801-970 Araraquara-SP, Brazil

^bDepartamento de Ciencia de Materiales e Ingeniería Metalúrgica, Universitat de Barcelona,
08028 Barcelona, Spain

Estudos eletroquímicos localizados de grãos individuais de uma liga policristalina Cu-16%Zn-8%Al foram realizados em solução de tampão borato (pH 8,4) por meio da técnica eletroquímica com microcapilar. As orientações dos grãos, determinadas pelo método de retro-reflexão de Laue, foram predominantemente próximas à direção [110], sugerindo uma texturização da amostra. As medidas de potencial em circuito aberto mostraram que o menor potencial de estado estacionário foi observado para o grão que possui o maior número de degraus na superfície da liga. Os experimentos de voltametria cíclica sugeriram que a orientação do Cu₂O segue a orientação do substrato na liga Cu-Zn-Al, enquanto que CuO cresce independentemente.

Local electrochemical studies of single grains of a polycrystalline Cu-16%Zn-8%Al alloy were investigated in borate buffer solution (pH 8.4) by means of microelectrochemical technique. The grain orientations, which were determined by the Laue back-reflection method, were predominantly close to [110] direction, suggesting that the sample was texturized. The open circuit potential measurements showed that the lower steady state potential was observed for the grain which has the highest number of steps on the alloy surface. The cyclic voltammetry experiments suggested that the orientation of Cu₂O follows the substrate one in the Cu-Zn-Al alloy, while CuO grows independently.

Keywords: Cu-Zn-Al alloys, shape memory alloys, single grains, borate buffer, microelectrochemical cell

Introduction

Since the discovery of shape memory effect (first in Au-Cd alloys and later in Ni-Ti ones)^{1,2} great effort and funds have been spent on the study of shape memory alloys (SMAs) by virtue of their attractive properties such as low cost, pseudoelasticity and two-way shape memory effect (TWSME).³⁻⁷ Cu-based and Ni-Ti alloys fill up these requisites, for instance. Owing to these unique properties, SMAs have been classified as “smart” or “intelligent” materials along with ferroelectric and piezoelectric ones.^{8,9} These materials exhibit a reversible transformation in macroscopic size which is controlled by changes of external conditions such as temperature, pressure or magnetic field.

In this context, SMAs have a myriad of applications in the engineering and medical fields including couplings, sensors, actuators, antennas for mobile phones,¹⁰ air conditioning systems,¹¹ active endoscopes and artificial muscle components for robotics.¹²

In this work, we report on the local electrochemical investigation of single grains of a polycrystalline Cu-16(wt.%)Zn-8(wt.%)Al alloy. Many studies have only described the fabrication, mechanical properties and physical characterization of SMAs, but electrochemical studies concerning Cu-Zn-Al alloys are hitherto scarce. Celis *et al.*¹³ focused on the corrosion behavior of austenite (β) and martensitic (β') Cu-Zn-Al alloys in different media. They observed that alloys containing more than 15 wt.% Zn may undergo a process called dezincification where Zn is leached out. According to their

*e-mail: benedeti@iq.unesp.br

data, at comparable zinc and aluminum contents, the β -alloy is less sensitive to dezincification than the β' structure.

Differently from single crystal materials, which have no grain boundaries, polycrystalline ones are composed of several grains varying in size and orientation. The role of each single grain is not detected by using surface-averaged techniques. Thus, the study and understanding of their activities (*e.g.*, electrochemical) in a local point of view are needed. Local electrochemistry via electrochemical microcell has been, and continues to be, extensively employed in numerous fields such as corrosion studies,¹⁴⁻¹⁶ batteries,¹⁷⁻¹⁹ electrodeposition²⁰⁻²² and biological environments.²³⁻²⁵ Besides local resolution, the use of electrochemical microcell has significant advantages compared to conventional one. In this sense, it may be cited the possibility of employing aggressive solutions, small wetted area and amounts of the electrolyte, small mechanical stress applied to the sample, among others.^{16,26} Therefore, this work is aimed to monitor the electrochemical activity of single grains on the surface of a polycrystalline Cu-Zn-Al alloy by means of microelectrochemical technique.

Experimental

The polycrystalline Cu-16(wt.%)Zn-8(wt.%)Al alloy was obtained by melting the metals with purity higher than 99.9% using an induction furnace from Inductotherm Power-Track under argon atmosphere in a graphite crucible. The melting temperature was about 1400 °C. The resulting ingot was machined to produce small discs (10 mm diameter and 5 mm thickness) that were annealed at 850 °C for 20 min under argon atmosphere in an EDGCOM 3P furnace. After that, the sample was promptly quenched to water at 100 °C and finally to water at 0 °C. This procedure was made in order to obtain the alloy containing the β -phase^{27,28} under room temperature conditions.

The alloy chemical analysis was determined using an atomic absorption spectrophotometer from Varian Intralab AA-1475. The results are shown in Table 1.

The samples were polished using SiC and diamond paste, etched and examined by optical and scanning electron microscopy (SEM). Optical and SEM images were obtained using a Leica DMR optical and a Jeol

JSM-T330A SEM microscope, respectively. X-ray diffraction (XRD) measurements were performed in the 2θ range of 10-100° with step size of 0.05° and step time of 5 s using a Siemens D5000 X-ray generator. $\text{CuK}\alpha$ (1.5418 Å) radiation was used at 40 kV and 30 mA with monochromator at the diffracted beam.

After a slight attack to reveal the sample surface using an etching solution (0.5 g FeCl_3 , 3 mL concentrated HCl, 3 mL isoamyl alcohol, 3 mL ethanol and 0.5 mL distilled water), the grains were marked with numbers to facilitate a posterior analysis. In order to determine the grain orientations, the Laue back-reflection method was used,²⁹⁻³² whose data were interpreted by utilizing a Greninger chart.

The electrochemical studies were carried out in a homemade microcell developed in our laboratory.³³ An overview of the experimental set-up utilized to perform the microelectrochemical measurements is shown in Figure 1. To facilitate the visualization of the desired area, the microcell was coupled to a Carl Zeiss optical microscope. The ground tip of the microcell could be varied from 20 to 600 μm in diameter. In all experiments, a 600 μm tip was used because it demonstrated to be the most appropriate to study the single grains.



Figure 1. Overview of the experimental set-up with electrochemical microcell (adapted from reference 33).

The employed electrochemical methods were open-circuit potential and cyclic voltammetry using an EG&G PAR Model 273A Potentiostat/Galvanostat, which was connected to an IBM-PC computer. The used electrolyte in all measurements was the borate buffer solution pH 8.4 containing 0.3 mol L⁻¹ H_3BO_3 and 0.075 mol L⁻¹ $\text{Na}_2\text{B}_4\text{O}_7$, prepared from analytical grade reagents (Merck) and Milli-Q water (18.2 M Ω cm). The volume for each experiment was 1 mL of a deaerated aqueous solution. The reference electrode was a Hg/HgO/ OH^- which was prepared according to the procedure previously described.³⁴

Table 1. Chemical composition of the polycrystalline Cu-Zn-Al alloy obtained by atomic absorption spectrophotometer

Element	wt.% (± 0.5)	at.% (± 0.5)
Cu	75.5	68.3
Zn	16.4	14.4
Al	8.10	17.3

The potential of this electrode vs. SHE is 0.431 V. A Pt wire was used as auxiliary electrode. In the cyclic voltammetry experiments, a 0.1 μF non-electrolytic capacitor connecting a Pt wire to the reference electrode was utilized in order to minimize noise. This avoids the reference electrode polarization and diminishes the ohmic drop.³⁵

Results and Discussion

Physical characterization

Figure 2 displays the SEM image of polycrystalline Cu-16(wt.%)Zn-8(wt.%)Al alloy after etching with an acid solution of FeCl_3 ³⁶ for 10 s. No lamellar structure or plate presence (typical of martensitic phase) is observed, indicating that the quenching process was effective, giving rise to an alloy containing only the β -phase. In fact, thermal treatments, such as quenching and annealing, applied to brass using high temperatures for long periods of time may cause dezincification to Cu-Zn-based alloys.³⁷ In addition, β -brasses (including the Cu-Zn-Al alloys) are known by presenting an excessive grain growth when submitted to heat treatments at temperatures corresponding to the single phase region.³⁸

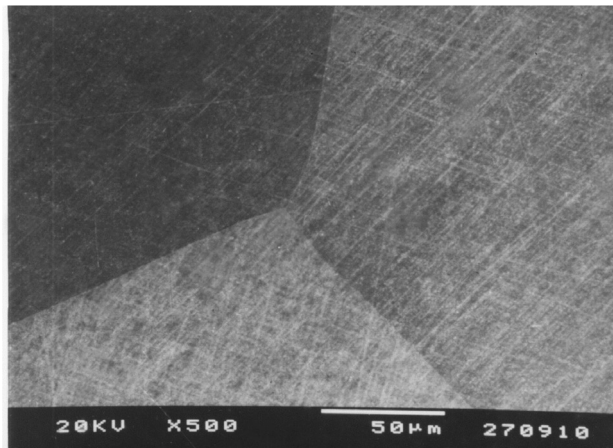


Figure 2. SEM image of polycrystalline Cu-16(wt.%)Zn-8(wt.%)Al alloy after etching for 10 s.

The existence of an alloy containing only the β -phase was also confirmed by XRD diffractogram as shown in Figure 3. The peaks referring to 40.35°, 42.22°, 44.14° and 46.01° were attributed to the β -phase. No other phases were noticed.

Determination of single grain orientations

Figure 4a depicts the optical micrograph of polycrystalline Cu-16(wt.%)Zn-8(wt.%)Al alloy obtained

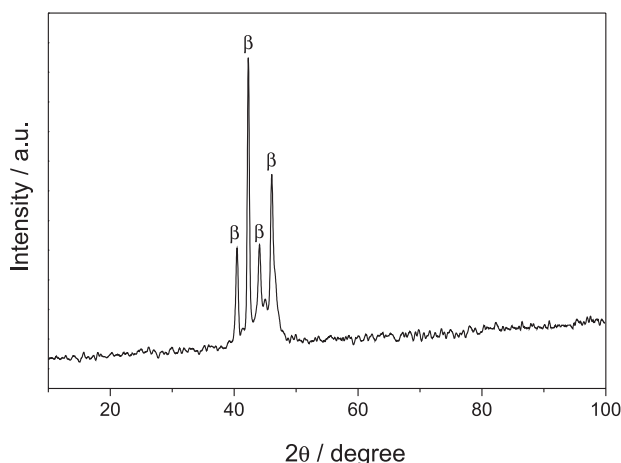


Figure 3. XRD pattern of polycrystalline Cu-16(wt.%)Zn-8(wt.%)Al alloy.

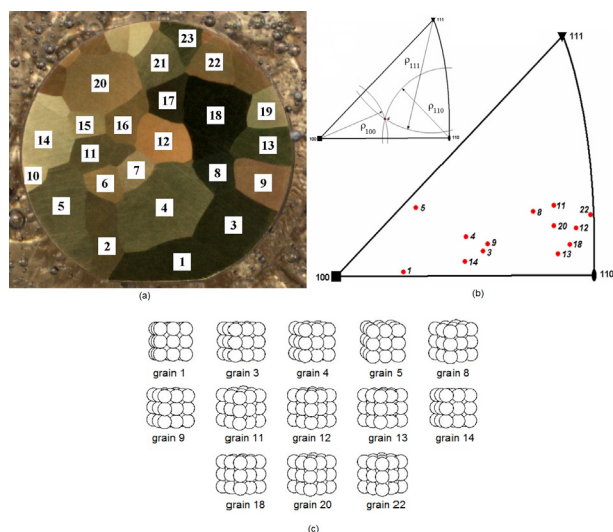


Figure 4. (a) Optical micrograph of polycrystalline Cu-16(wt.%)Zn-8(wt.%)Al alloy obtained by petrographic microscopy (the single grains were numbered from 1 to 23), (b) fundamental triangle indicating the orientation of different single grains of the Cu-Zn-Al alloy and (c) schematic view of the relative position of single grains on the surface of the Cu-Zn-Al alloy. (Adapted from reference 33).

by petrographic microscopy. It can be noticed different grains varying in size and shape. By virtue of the alloy cubic symmetry, the stereographic projection can be divided in 24 similar and equivalent triangles, each one possessing $\{100\}$, $\{110\}$ and $\{111\}$ forms. In this sense, the grain orientations are better indicated by ρ_{100} , ρ_{110} and ρ_{111} angles referring to the plane slope with respect to the low Miller index planes $[(100)$, (110) and $(111)]$, respectively. Table 2 shows the ρ_{100} , ρ_{110} and ρ_{111} values found for the different single grains of Cu-16(wt.%)Zn-8(wt.%)Al alloy that were projected into a fundamental triangle illustrated in Figure 4b. A schematic view of the relative position of each single grain on the surface of the alloy is shown in Figure 4c. It is seen that most of the grains are located

Table 2. ρ_{hkl} values found for the different single grains of Cu-16(wt.%Zn-8(wt.%Al alloy which were projected into a fundamental triangle

Grain	ρ_{100} / degree	ρ_{110} / degree	ρ_{111} / degree
1	12	33	48
3	27	19	36
4	24	22	35
5	18	32	36
8	37	14	27
9	28	19	36
11	40	12	26
12	43	7	29
13	40	7	36
14	23	22	40
18	41	5	32
20	40	10	30
22	46	8	27

close to the [110] direction, suggesting that the sample is texturized. According to Yuan *et al.*,³⁹ the austenite (β -phase) presence in polycrystalline Cu-Zn-Al alloys exhibits texture with respect to the [110] direction. The knowledge about texture in polycrystalline SMAs such as Cu-Zn-Al alloys is of great interest because it is intrinsically related to the plasticity of the phase transformation.³⁹

Electrochemical measurements: open circuit potential and voltammetry

Figure 5a displays the open circuit potential measurements (E_{oc} curves) obtained for the single grains of polycrystalline Cu-16(wt.%Zn-8(wt.%Al alloy in borate buffer solution pH 8.4. A difference of about 40 mV was noticed among the curves, indicating that the alloy stability in this medium depends on the crystallographic orientation. The lower steady state potential was observed for the grain 5 which is most likely affected by its higher number of steps (64) on the alloy surface. After the E_{oc} curves, it was recorded the linear voltammograms of each single grain, scanning the potential in the direction of the oxides reduction, which were formed on the surface (Figure 5b). It is seen a low intensity peak at -0.58 V/Hg/HgO/OH⁻ for the grain 1, while for the grain 13 this peak appears at -0.72 V/Hg/HgO/OH⁻. The voltammogram for the grain 4 shows a reduction peak at *ca.* -1.0 V/Hg/HgO/OH⁻. The grain 5 does not have reduction peak and the grain 22 depicts a well-defined peak at -0.80 V/Hg/HgO/OH⁻. All of these peaks are probably owing to the reduction of copper(I) oxides, which were

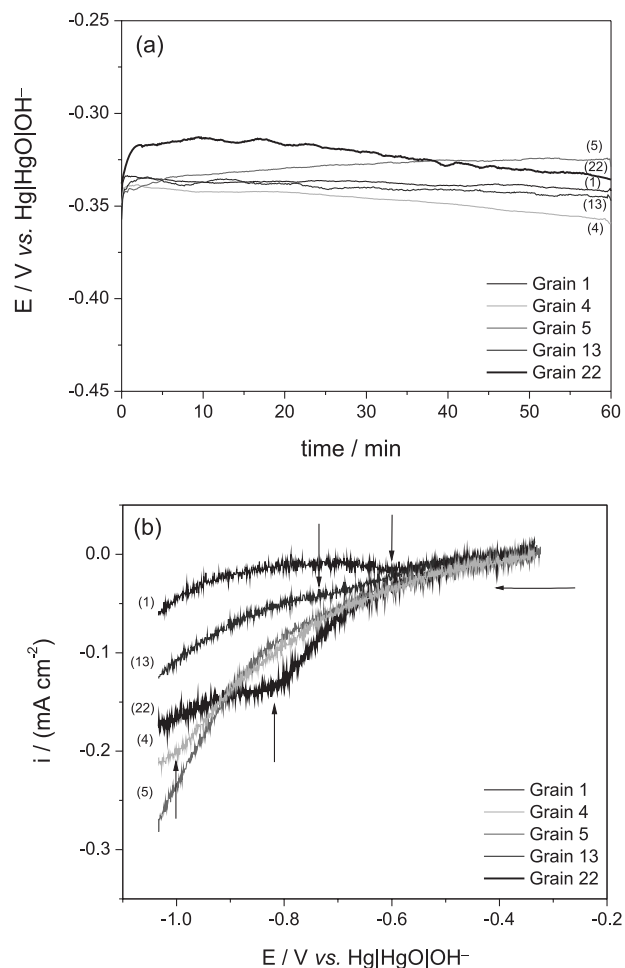


Figure 5. (a) Open circuit potential measurements for single grains of polycrystalline Cu-16(wt.%Zn-8(wt.%Al alloy and (b) linear voltammograms at $v = 20$ mV s⁻¹ (highlighting the reduction of oxides formed at open circuit). Both plots were obtained in the borate buffer electrolyte at pH 8.4.

formed in the exposure of the grains to the electrolyte. This evidences that the amount and stability of the oxide film are dependent on the crystallographic orientation.

Figure 6 shows the cyclic voltammograms for different single grains of the polycrystalline Cu-16(wt.%Zn-8(wt.%Al alloy obtained with a scan rate (v) of 20 mV s⁻¹. The main difference observed in all cases concerns the reduction region of Cu₂O to Cu. Scanning tunneling microscopy (STM) studies for single crystal Cu (111) and Cu (001) in 0.1 mol L⁻¹ NaOH showed that Cu₂O formation obeys the substrate orientation, while CuO grows independently of it.^{40,41} In this sense, the cuprous oxide grew onto Cu (111) following the substrate orientation and leading to Cu₂O (111) formation, similarly the Cu₂O (001) one. However, it is noticed that the cupric oxide does not obey the substrate orientation and thus it is orientated in both cases in CuO (001). Therefore,

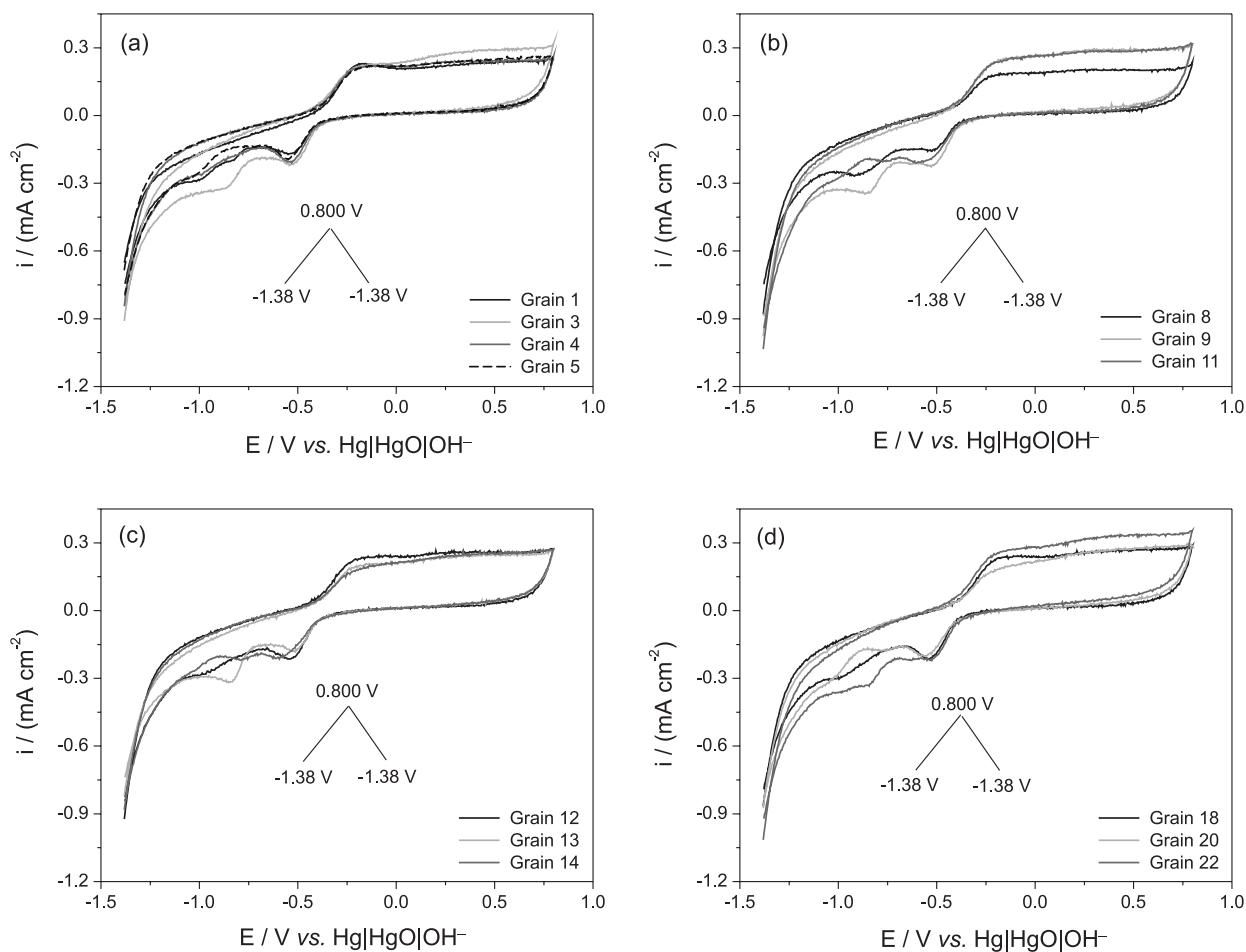


Figure 6. Cyclic voltammograms of single grains of polycrystalline Cu-16(wt.%)Zn-8(wt.%)Al alloy in borate buffer solution pH 8.4 and $\nu = 20 \text{ mV s}^{-1}$.

it is suggested that the orientation of Cu_2O follows the substrate one also in the Cu-Zn-Al alloy and this may be the main feature of the differences observed by cyclic voltammograms for the single grain.

The i - E profiles presented in Figure 6 indicate that the cupric oxide grows independently of the substrate orientation. Due to this fact, the current peak corresponding to its reduction does not significantly alter as the grain orientation is modified. By contrast, the regions with respect to the formation and reduction of cuprous oxide seem to be more influenced by the grain orientation. In this case, it is noticed a variation in the anodic current and also in the presence of multiple reduction peaks that are dependent on the grain orientation. In order to confirm this observation, cyclic voltammograms (Figure 7) were recorded using an anodic scan up to the positive limit of Cu_2O formation potential followed by the cathodic scan. It is verified in all cases that the potential and the current density of the reduction peaks, which are attributed to the Cu_2O reduction, present values considerably different. These differences are better understood when the current

densities taken at $-0.13 \text{ V/Hg/HgO/OH}^-$ (the switching potential) are analyzed. At this potential value, the anodic peak essentially represents the copper oxidation to cuprous oxide (Cu_2O). Assuming that oxide is also formed on the surface during the alloy etching, it would diminish the anodic current value at about $-0.13 \text{ V/Hg/HgO/OH}^-$. Hence, it would be expected that grains with orientations close to the plane (110) would more easily oxidize during the etching and consequently, they give rise to low current densities at $-0.13 \text{ V/Hg/HgO/OH}^-$ (as observed for the grains 12, 18 and 20). In this context, the anodic current densities at $-0.13 \text{ V/Hg/HgO/OH}^-$ were correlated to the ρ_{100} , ρ_{110} and ρ_{111} values which are the angles between the grain orientation and the main low Miller index planes. These data are summarized in Table 3.

It is noticed that an increase in ρ_{110} value (and in lower magnitude in ρ_{111}) results in current density increase as well. On the other hand, an augment in ρ_{100} gives rise to a current density diminishing. This plane has the lowest atomic density in comparison to the other two ones.

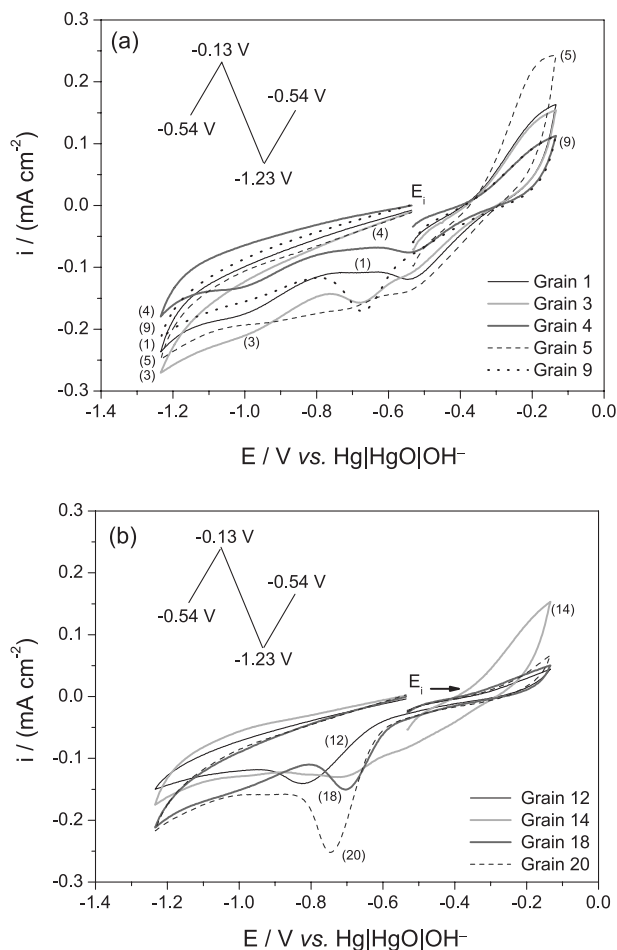


Figure 7. Cyclic voltammograms of single grains of polycrystalline Cu-16(wt.%)Zn-8(wt.%)Al alloy in borate buffer solution pH 8.4 and $v = 20 \text{ mV s}^{-1}$ (emphasizing the region of Cu oxidation to Cu_2O) (adapted from reference 33).

Table 3. Current densities at $-0.13 \text{ V}/\text{Hg}/\text{HgO}/\text{OH}^-$ (reversal potential) and ρ_{hkl} values for single grains of polycrystalline Cu-16(wt.%)Zn-8(wt.%)Al alloy

Grain	$i / (\text{mA cm}^{-2})$	$\rho_{100} / \text{degree}$	$\rho_{110} / \text{degree}$	$\rho_{111} / \text{degree}$
1	0.163	12	33	48
3	0.154	27	19	36
4	0.112	24	22	35
5	0.243	18	32	36
9	0.112	28	19	36
12	0.044	43	7	29
14	0.153	23	22	40
18	0.050	41	5	32
20	0.067	40	10	30

Conclusions

The local electrochemical studies of single grains of polycrystalline Cu-16(wt.%)Zn-8(wt.%)Al alloy in

borate buffer solution were fruitfully performed by using an electrochemical microcell. The single grains exhibited texture with a preferred orientation close to (110) plane. In general, the alloy electrochemical behavior displayed a dependence of the crystallographic orientation of each single grain. The grains, whose orientations are more distant of the low Miller index planes, presented a more active surface, being possibly related to its higher number of atomic steps.

Acknowledgements

The authors gratefully acknowledge financial support and scholarships from the Brazilian funding agencies Fundação de Apoio à Pesquisa do Estado de São Paulo (FAPESP, proc. No. 2004/11984-2) and Conselho Nacional de Desenvolvimento Científico e Tecnológico (CNPq, proc. No. 305890/2010-7).

References

- Chang, L. C.; Read, T. A.; *Trans., AIME* **1951**, *189*, 47.
- Buehler, W. J.; Gilfrich, J. W.; Wiley, R. C.; *J. Appl. Phys.* **1963**, *34*, 1475.
- Li, Z.; Pan, Z. Y.; Tang, N.; Jiang, Y. B.; Liu, N.; Fang, M.; Zheng, F.; *Mater. Sci. Eng., A* **2006**, *417*, 225.
- Xiao, Z.; Li, Z.; Fang, M.; Xiong, S.; Sheng, X.; Zhou, M.; *Mater. Sci. Eng., A* **2008**, *488*, 266.
- Zak, G.; Kneissl, A. C.; Zatulskij, G.; *Scr. Mater.* **1996**, *34*, 363.
- Serra, G. C.; Benedetti, A. V.; Noce, R. D.; *J. Braz. Chem. Soc.* **2010**, *21*, 1530.
- Fernandez, J.; Zhang, X. M.; Guilemany, J. M.; *J. Mater. Process. Technol.* **2003**, *139*, 117.
- Adiguzel, O.; *J. Mater. Process. Technol.* **2007**, *185*, 120.
- Ciatto, G.; Solari, P. L.; De Panfilis, S.; Fiorini, A. L.; Amadori, S.; Pasquini, L.; Bonetti, E.; *Appl. Phys. Lett.* **2008**, *92*, 241903.
- Otsuka, K.; Kakeshita, T.; *MRS Bull.* **2002**, *27*, 91.
- Todoroki, T.; *Met. Technol.* **1984**, *54*, 2.
- Madden, J.; *Science* **2006**, *311*, 1559.
- Celis, J. P.; Roos, J. R.; Terwinghe, F.; *J. Electrochem. Soc.* **1983**, *130*, 2314.
- Suter, T.; Böhni, H.; *Electrochim. Acta* **1998**, *43*, 2843.
- Kobayashi, Y.; Virtanen, S.; Böhni, H.; *J. Electrochem. Soc.* **2000**, *147*, 155.
- Andreatta, F.; Matesanz, L.; Akita, A. H.; Paussa, L.; Fedrizzi, L.; Fugivara, C. S.; Salazar, J. M. G.; Benedetti, A. V.; *Electrochim. Acta*, **2009**, *55*, 551.
- Verbrugge, M. W.; Koch, B. J.; *J. Electroanal. Chem.* **1994**, *367*, 123.
- Ura, H.; Nishina, T.; Uchida, I.; *J. Electrochem. Soc.* **1995**, *396*, 169.

19. Kostecki, R.; McLarnon, F.; *Electrochem. Solid-State Lett.* **2004**, *7*, A380.
20. De Abril, O.; Mandler, D.; Unwin, P. R.; *Electrochem. Solid-State Lett.* **2004**, *7*, C71.
21. Sheffer, M.; Mandler, D.; *Electrochim. Acta* **2009**, *54*, 2951.
22. Lin, J. C.; Chang, T. K.; Yang, J. H.; Chen, Y. S.; Chuang, C. L.; *Electrochim. Acta* **2010**, *55*, 1888.
23. Wightman, R. M.; *Anal. Chem.* **1981**, *53*, 1125A.
24. Pons, S.; Fleischmann, M.; *Anal. Chem.* **1987**, *59*, 1391A.
25. Chen, T. K.; Lau, Y. Y.; Wong, D. K. Y.; Ewing, A. G.; *Anal. Chem.* **1992**, *64*, 1264.
26. Lohrengel, M. M.; Moehring, A.; Pilanski, M.; *Electrochim. Acta* **2001**, *47*, 137.
27. Satto, C.; Jansen, J.; Lexcellent, C.; Schryvers, D.; *Solid State Commun.* **2000**, *116*, 273.
28. Baker, H.; Okamoto, H.; *ASM Handbook, Alloy Phase Diagrams*, vol. 3; ASM International: USA, 1992, p. 3.13.
29. Warren, B. E.; *J. Appl. Phys.* **1941**, *12*, 375.
30. Cullity, B. D.; *Elements of X-ray Diffraction*; Reading, Mass., Addison-Wesley Pub. Co.: Massachusetts, 1956, ch. 8.
31. ASTM E82-91: *Standard Test Method for Determining the Orientation of a Metal Crystal*, ASTM International, West Conshohocken, PA, 1996.
32. Zambrano, U. C.; Blanco, M.; Barelli, N.; Benedetti, A. V.; Fernández, J.; *Quim. Nova* **2008**, *31*, 154.
33. Akita, A. H.; Barragan, J. T. C.; Fugivara, C. S.; Benedetti, A. V.; *Quim. Nova*, in press.
34. Ives, D. J. G.; Janz, G. J.; *Reference Electrodes: Theory and Practice*; Academic Press: New York, 1961.
35. Garreau, D.; Saveant, J. M.; Binh, S. K.; *J. Electroanal. Chem.* **1978**, *89*, 427.
36. Ricksecker, R. E.; Bower, T. F.; *Metallography and Microstructures: Copper and Copper Alloys*, vol. 9; American Society for Metals Handbook, Metals Park: Ohio, 1985, p. 399.
37. Giacobbe, F. W.; *J. Alloys Compd.* **1993**, *202*, 243.
38. Gil, F. J.; Guilemany, J. M.; Fernandez, J.; *Mater. Sci. Eng., A* **1998**, *241*, 114.
39. Yuan, W. Q.; Wang, J. N.; *J. Mater. Process. Technol.* **2002**, *123*, 31.
40. Kunze, J.; Maurice, V.; Klein, L. H.; Strehblow, H. H.; Marcus, P.; *J. Electroanal. Chem.* **2003**, *554*, 113.
41. Kunze, J.; Maurice, V.; Klein, L. H.; Strehblow, H. H.; Marcus, P.; *Corros. Sci.* **2004**, *46*, 245.

Submitted: June 17, 2011

Published online: September 8, 2011

FAPESP has sponsored the publication of this article.